1-A and-120 mA Thin-Film Multijunction Thermal Converters

Héctor Laiz, Thomas F. Wunsch, *Senior Member, IEEE*, Joseph R. Kinard, and Thomas E. Lipe

Abstract—We report on the development of thin-film multijunction thermal converters for the measurement of ac currents up to 10 A without relying on parallel current shunts. The materials and designs chosen for these devices have been optimized to provide high accuracy over a wide range of input levels and frequencies. Preliminary measurements on a 10-A chip made with a copper–gold heater indicate that its ac–dc difference is nearly zero from 10 Hz to 100 kHz, and that the ac–dc difference is independent of input current level.

Index Terms—AC–DC difference, current converter, thermal converter, thermal current converter, thermoelement.

I. INTRODUCTION

THIN-FILM multijunction thermal converters (MJTCs) exhibit small ac–dc transfer differences in the frequency range from 10 Hz to 1 MHz. As thermal current converters, they may be used as standards for current up to 10 mA [1]. For higher currents, parallel shunts may be used [2], but they present problems from both stray capacitances to ground and thermal drifts, and exhibit greater errors from skin effect at 20 kHz and above. The goal of the present work is to realize the ac–dc current scale up to 10 A, while avoiding the use of shunts. This realization is based on 1-A and 120-mA MJTCs, which in parallel combinations can be used to scale currents up to 10 A [3]. The proposed parallel combinations of MJTCs are shown in Table I.

By eliminating the shunt and its mounting structure, MJTCs offer the following advantages.

1) MJTCs can have a lower voltage drop across the heater of the converter (0.1 V at rated input current) since the voltage need not be measured by a thermoelement (TE) or voltmeter. This limits the heat produced and reduces the temperature-dependent errors. It also reduces the current through parasitic capacitances.

2) MJTCs can have a small skin effect at high frequencies, reducing the high-frequency error.

3) MJTCs require no parallel impedance (as with a shunt) and offer a higher impedance to ground.

TABLE I
COMBINATIONS OF MJTCs REQUIRED TO SCALE THE AC–DC DIFFERENCE FOR CURRENT FROM 100 mA TO 10 A (NOTE THAT 10 A WILL BE APPLIED TO THE 8 A COMBINATION)

Single MJTC	2 in parallel	4 in parallel	8 in parallel
120 mA	240 mA	480 mA	1 A
1 A	2 A	4 A	8 A

4) The larger output EMFs possible with MJTCs enhance the accuracy of current scaling by increasing the usable input current range.

II. DESIGN OF THE 1-A MJTC

At the beginning of the design process, tradeoffs were made among the low voltage desired across the heater, the dissipated power, the characteristics of the heater alloy, and the size of the chip. For the desired voltage drop across the heater of 0.1 V at 1 A, this results in 100 mW of power in the heater, or about five to ten times the power dissipated in common MJTCs. Dissipating this power in a $0.1\text{-}\Omega$ thin-film heater requires both a new chip design and the selection of an appropriate low-resistivity alloy.

A. Heater Alloy

Low-resistivity metals and alloys exhibit high temperature coefficients of resistivity. This temperature coefficient plays a crucial role in the temperature coefficient of the sensitivity. The sensitivity, S, can be calculated as

$$S = N\frac{U_0}{P_J} = N\frac{\alpha_{\frac{A}{B}}\Delta T}{P_{J0}(1+\alpha T)} = N\frac{\alpha_{\frac{A}{B}}}{G_T}(1-\alpha T) \quad (1)$$

where N is the number of thermocouples, U_o is the output voltage, P_J the joule heat in the heater, $\alpha_{A/B}$ the Seebeck coefficient of the thermocouples, ΔT the temperature rise of the hot junctions, G_T the total thermal conductance of the device, P_{Jo} the joule heat for the heater resistance at ambient temperature, α the temperature coefficient of the heater resistance, and T the ambient temperature. The temperature coefficient, β_S, of the sensitivity is

$$\beta_S = \frac{1}{S}\frac{\partial S}{\partial T} \approx \frac{1}{\alpha_{\frac{A}{B}}}\frac{\partial \alpha_{\frac{A}{B}}}{\partial T} - \frac{1}{G_T}\frac{\partial G_T}{\partial T} - \alpha. \quad (2)$$

For a thermal converter that will be used only as a current converter, the temperature coefficient of the resistivity can be used to compensate for the difference in the temperature coefficient of the Seebeck coefficient and the total thermal conductance. It is easily shown that this compensation will not work properly if
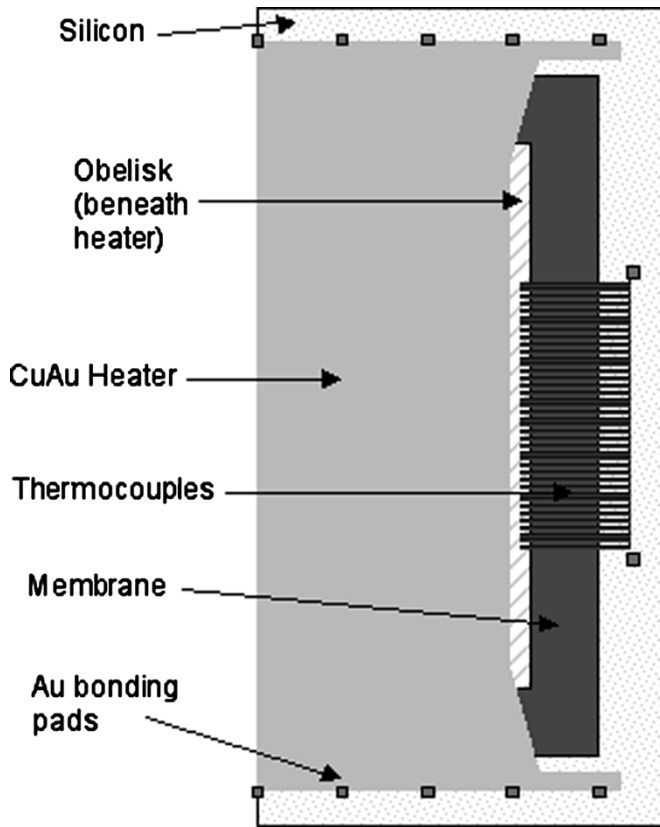
Fig. 1.   Layout of one-half of the 1-A chip. The various structures are noted.

Fig. 2.   Temperature distribution on one-half of the 1 A-chip.

Fig. 3.   Temperature profile along the heater on the obelisk of the 1-A chip.

the same device is used as a voltage converter. Previously fabricated MJTCs with gold heaters show a β_S of $+3.2 \times 10^{-3}$ K^{-1} compared to -6.0×10^{-4} K^{-1} for those with Evanohm heaters. This difference agrees with the temperature coefficient of resistivity for gold. To achieve an optimum β_S for the 0.1-Ω heater, we selected a copper–gold alloy (80% Cu to 20% Au) that has a resistivity of 5.3×10^{-8} $\Omega \bullet$ m at 293 K, and α of 1.1 $\times$ 10^{-3} K^{-1}. One ampere devices with this alloy show a β_S of -2.5×10^{-4} K^{-1}. This improves the stability of the output voltage and reduces the ac–dc differences at low frequencies [4].

B. Thermal Design

The low-current chip [3] dissipates 20 mW in the heater. To achieve approximately the same temperature rise in the 1-A heater with 100 mW dissipated, the chip geometry was dramatically changed. Fig. 1 shows the 1-A design. The dimensions of the membrane are 5 × 5 mm, the obelisk (a silicon structure left beneath the heater to increase the thermal time constant and reduce low-frequency errors) is 4 × 4 mm and the heater 5 mm × 3.8 mm × 1 μm. These design changes reduce the sensitivity (i.e., increase the thermal conductance.) Thus, we designed a narrower membrane and made the surfaces of the heater and obelisk larger to dissipate the heat. An additional constraint is the size of the heater necessary to achieve a resistance of 0.1 Ω.

The new design was modeled and optimized using finite element analysis. All the nonlinearities in the material parameters and radiation were included in the model. Fig. 2 shows the
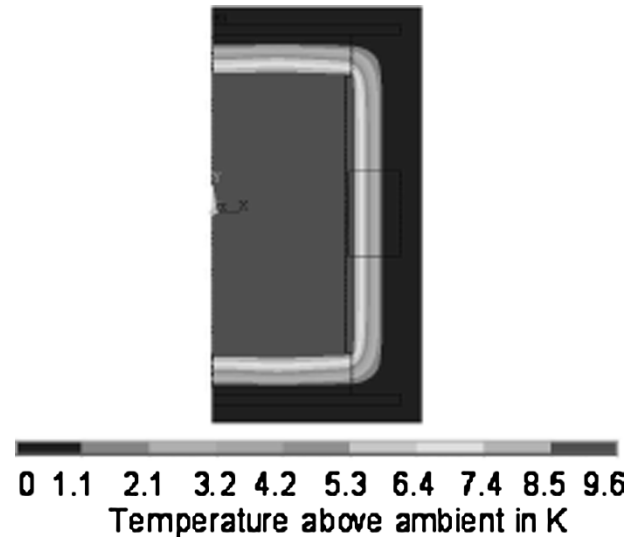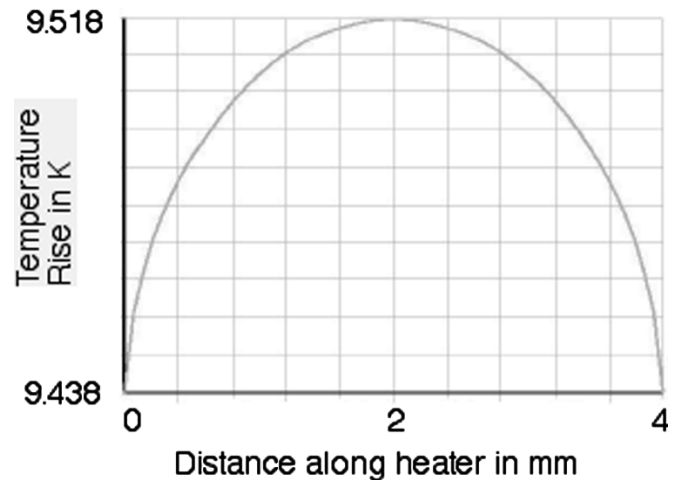
simulation of the temperature distribution on the membrane. Most of the heat is conducted though the heater itself due to its high thermal conductance arising from the high conductivity and large cross section. Consequently, the simulation indicated that the ratio of the sensitivity in air to the sensitivity in vacuum is only 1.5.

Thomson and Peltier effects are the main source of ac–dc difference in the audio frequency range. Simulations of the Thomson heat indicate that it has a negligible effect on the temperature of the heater. The temperature gradient across the heater on the obelisk is quite small. Fig. 3 shows the results of the thermal simulation of the temperature profile along the edge of the heater on the obelisk. The temperature difference is less than 90 mK. Although the heater alloy has not been optimized for a small Thomson coefficient, the low temperature gradient reduces the Thomson heat.

The Peltier effect was included in the simulation as a heat source at the connection between the pads (Au) and the heater (CuAu). Results show no influence from the Peltier heat on the temperature of the heater on the obelisk. As the influence of the

TABLE II
MEASURED AC–DC DIFFERENCES IN $\mu A / A$ WITH 1 A APPLIED. UNCERTAINTIES ARE $k = 2$

	10 Hz	100 Hz	1 kHz	10 kHz	20 kHz	100 kHz
MJTC	-3.3 ± 20	-4.9 ± 12	+0.4 ± 12	+4.0 ± 12	-2.5 ± 12	+4.7 ± 26
TE	+41.4 ± 20	-7.0 ± 12	-7.0 ± 12	-8.8 ± 12	-11.4 ± 12	-55.6 ± 26

thermoelectric effects is so small, the number of the thermocouples was doubled (to 40 per side) in the second fabrication run in order to increase the output voltage.

The connection track between the two arms of the thermocouples was removed from the chip and made externally in order to reduce the capacitance between heater and thermocouples. If this connection is made on the chip, the ac–dc difference at high frequencies depends upon which terminal of the heater is at high potential.

C. Measurement Results

Thermal converters were fabricated in accord with the design described above. They typically show time constants of 0.5 to 0.7 s, and a reversal difference of about 10 μA/A or less. The measured ac–dc differences for a representative MJTC with an input current of 1 A is presented in Table II, along with the ac–dc differences of the present NIST reference standard current transfer TE for comparison. These measurements agree well with simulated results.

The performance of the new 1-A MJTC is also much better than commercially available combinations of shunts and single-junction thermal converters, which typically have ac–dc differences of several tens of μA/A at 10 Hz, and ac–dc differences of up to several hundred μA/A at 100 kHz.

III. 120-mA CONVERTER DESIGN

The same chip layout used for the 1-A MJTC was used for the 120-mA design, but Evanohm[1] was used as the heater material. Several performance issues were noted with this design. The 1-A chip was intended to dissipate 100 mW of power. This 120-mA chip required a voltage drop of 833 mV to dissipate the same power with approximately the same temperature rise in the hot junctions of the thermocouples. This relatively high voltage increases the ac–dc difference produced by the leakage capacitance at high frequency. The design goal is to maintain a voltage drop in the heater of about 100 mV at 120 mA, requiring a heater resistance of 0.83 Ω. In this design, the input power will be 12 mW. To achieve these design goals, we propose to use the basic design of the previously reported 400-Ω chip [5], with three modifications:

1) The connection between the two arms of the thermocouples should be removed from the chip and the series connection made outside the chip package to reduce coupling into the heater circuit.

0   0.8   1.7   2.5   3.4   4.2   5.1   5.9   6.8   7.6
Temperature above ambient in K

Fig. 4.   Temperature distribution on one-half of the 120-mA chip.

2) The thermocouples should be placed at a distance of 10 μm from the edge of the silicon obelisk to reduce the capacitance.
3) The heater should be made of CuAu, and have the following dimensions: a thickness of 1 μm, a width of 220 μm, and a length of 3000 μm.

Fig. 4 shows the simulation of the temperature distribution on the membrane. In air, the output voltage is 20 mV, with a temperature coefficient of 1×10^{-3} K^{-1}. The influences of Peltier and Thomson Effects were also calculated and found to be negligible.

IV. CONCLUSION

New 1-A thin-film MJTCs have been designed and fabricated. A finite element model that includes all nonlinear parameters was used to calculate the influence of thermoelectric effects on the performance of the MJTCs and to choose the appropriate material for the heater. Measurements on the 1-A MJTCs show that the new converters may be used to establish a new ac–dc current scale up to 10 A, without relying on parallel current shunts. Results from the 1-A MJTCs are guiding the development of 120-mA MJTCs. It is anticipated that the performance of these new devices will result in a reduction of the uncertainties in the NIST calibration service for ac current, and may lead to improvements in the services that rely on ac–dc difference metrology.

[1]Certain commercial entities, equipment, or materials may be identified in this document in order to describe an experimental procedure or concept adequately. Such identification is not intended to imply recommendation or endorsement by the National Institute of Standards and Technology, nor is it intended to imply that the entities, materials, or equipment are necessarily the best available for the purpose.
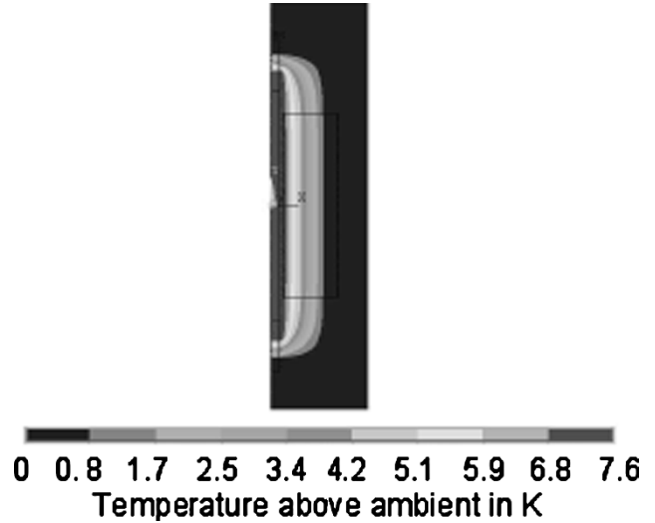
REFERENCES

[1] M. Klonz, H. Laiz, T. Spiegel, and P. Bittel, "ac–dc current transfer step-up and step-down calibration and uncertainty calculation," *IEEE Trans. Instrum. Meas.*, vol. 51, no. 5, pp. 1027–1034, Oct. 2002.

[2] J. R. Kinard, T. E. Lipe, and C. B. Childers, "ac–dc difference relationships for current shunt and thermal converter combinations," *IEEE Trans. Instrum. Meas.*, vol. 40, no. 2, pp. 352–355, Apr. 1991.

[3] J. R. Kinard, T. Lipe, and T. Wunsch, "Improved high-current thin-film multijunction thermal converters," in *Proc. CPEM Dig.*, Jun. 2002, pp. 364–365.

[4] H. Laiz, M. Klonz, E. Kessler, and T. Spiegel, "New thin-film multijunction thermal converters with negligible low-frequency ac–dc transfer differences," *IEEE Trans. Instrum. Meas.*, vol. 50, no. 2, pp. 333–337, Apr. 2001.

[5] T. Wunsch, J. R. Kinard, R. P. Manginell, O. M. Solomon, T. E. Lipe, and K. Jungling, "A new fabrication process for planar thin-film multijunction thermal converters," *IEEE Trans. Instrum. Meas.*, vol. 50, no. 2, pp. 330–332, Apr. 2001.